Methane Activation

DOI: 10.1002/anie.200905643

Methane Activation and Catalytic Ethylene Formation on Free Au_2^+**

Sandra M. Lang, Thorsten M. Bernhardt, Robert N. Barnett, and Uzi Landman**

Practical interest in the catalytic activation and conversion of methane into valuable products, such as methanol, formaldehyde, or light olefins, and in particular ethylene, is driven by industrial and economical considerations, and has motivated extensive research aimed at the identification and development of heterogeneous catalyst materials for these processes.[1] However, the required high reaction temperatures and/or the use of highly active reactants to activate the stable C–H bond of methane (bond dissociation energy 440 kJ mol^{-1} [2]) renders a selective synthesis of the desired products difficult. As pointed out in a recent Review,[3] the selective catalytic functionalization of C(sp^3)–H bonds in general poses a long-standing central problem in organometallic chemistry which is still unsolved. The complexity of these processes suggests that molecular-level insights into the methane-activation mechanism would be necessary for a successful formulation and implementation of versatile and selective catalytic reaction routes. Toward this goal we have embarked on a joint experimental and theoretical investigation of free metal clusters as catalytic model systems, with the expectation that these judiciously selected systems will allow us to gain fundamental understanding of the pertinent catalytic processes, while alleviating some of the complications that accompany other model systems, particularly supported catalysts.[4]

A growing body of experimental and theoretical research results, accumulated over the past decade, pertaining to the chemical reactivity and catalytic activity of gold that emerges at particle sizes reduced to nanometer-scale dimensions, has brought a paradigm shift regarding the chemical properties of gold, which until not too long ago has been viewed as the noblest of all metals.[5,6] In particular, it has been shown that size-selected gold nanoclusters containing approximately 10 atoms (about 1 nm in size) exhibit enhanced chemical activity (e.g., catalyzing the low-temperature oxidation of CO) when supported on metal oxides[7] or as charged gas-phase clusters.[8] However, investigations of methane activation on atomic gas-phase transition-metal ions[9] have concluded that the Au^+ ion is one of the few 5d metals found to be unreactive under thermal conditions.[10]

Investigations of methane activation involving free metal clusters are scarce. Whereas small platinum clusters Pt_x^+ were shown to exhibit facile activation and dehydrogenation of even multiple CH_4 molecules,[11] Au_x^+ ions were reported to be completely unreactive towards CH_4 under single-collision gas-phase conditions.[12] Yet, under multiple-collision conditions, reaction products could be stabilized and an uptake of several methane molecules was detected, but there was no indication for the dehydrogenation of CH_4.[13]

Herein we report temperature-dependent radio-frequency (RF) ion-trap mass-spectrometry measurements and first-principles theoretical calculations, revealing low-temperature activation and dehydrogenation processes of methane that lead to selective ethylene formation on free Au_2^+ ions in a full thermal catalytic cycle. Furthermore, we provide molecular level insights into a novel single-step catalytic C–C bond formation mechanism in this model catalytic system.

Figure 1 a–d displays product-ion mass distributions of the cationic gold dimer Au_2^+ exposed to methane at four different temperatures; labeling experiments with deuterated methane resulted in ion mass distributions exhibiting the expected shifts, confirming our peak assignments and excluding interference from background gases. At 200 K (Figure 1 a) the reaction proceeds fast yielding as main products $Au_2(CH_4)_2^+$ and $Au_2(CH_4)_3^+$ with two and three adsorbed methane

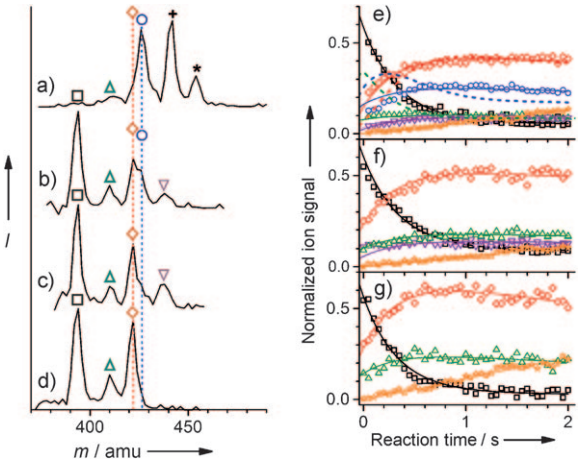

Figure 1. Temperature-dependent product-ion mass distributions and kinetics of the reaction of Au_2^+ with CH_4. Mass spectra have been recorded after trapping Au_2^+ for 0.1 s inside the ion trap at a) 200 K, b) 250 K, c) 270 K, and d) 300 K. The corresponding reaction kinetics were obtained at e) 250 K (0.04 Pa CH_4; 1.02 Pa He), f) 270 K (0.04 Pa CH_4; 1.0 Pa He), and g) 300 K (0.08 Pa CH_4; 0.96 Pa He). See text for details. □ Au_2^+; △: $Au_2(CH_4)^+$, ◇: $Au_2(C_2H_4)^+$, ○: $Au_2(CH_4)_2^+$, ▽: $Au_2(C_2H_4)(CH_4)^+$, ✲: $Au(C_2H_4)(CH_4)^+$, +: $Au_2(CH_4)_3^+$, ✳: $Au_2(C_4H_{12})^+$.

[*] Dr. S. M. Lang, Prof. Dr. T. M. Bernhardt
Institute of Surface Chemistry and Catalysis, University of Ulm
Albert-Einstein-Allee 47, 89069 Ulm (Germany)
Fax: (+49) 731-50-25452
E-mail: thorsten.bernhardt@uni-ulm.de
Dr. R. N. Barnett, Prof. Dr. U. Landman
School of Physics, Georgia Institute of Technology
Atlanta, Georgia 30332-0430 (USA)
Fax: (+1) 404-894-7747
E-mail: uzi.landman@physics.gatech.edu

[**] S.M.L. and T.M.B. acknowledge financial support by DFG and FCI. In particular, S.M.L. is grateful for a Kekulé fellowship of the FCI. R.N.B. and U.L. acknowledge support by the Air Force Office for Scientific Research (AFOSR) and the Department of Energy (DOE).

molecules, respectively, along with a low intensity product having a mass of 454 amu, corresponding to a complex that may be written as $Au_2(C_4H_{12})^+$. The stoichiometry of the complex suggests that rather than being composed simply of multiple CH_4 units, the adsorption of the methane molecules on the cluster leads to activation that results in the liberation of H_2 and subsequent formation of larger hydrocarbons; the methane activation capability of Au_2^+ is even more pronounced at higher temperatures (see below).

Heating the ion trap to 250 K decelerates the reaction and, moreover, changes entirely the observed ion mass distribution (Figure 1b). The 200 K products $Au_2(CH_4)_3^+$ and $Au_2(C_4H_{12})^+$ are not detected anymore, while $Au_2(CH_4)^+$ and $Au_2(CH_4)_2^+$ are present. Yet, the mass signal corresponding to $Au_2(CH_4)_2^+$ (426 amu, Figure 1 ○) is only a shoulder of a more intense signal at 422 amu which can be assigned to $Au_2(C_2H_4)^+$ (Figure 1 ◇). This result indicates that upon reaction with a second CH_4 molecule dehydrogenation through the release of two H_2 molecules occurs, potentially leading to the formation of ethylene on the gold dimer (see theoretical simulations below). An additional new product, $Au_2(C_2H_4)(CH_4)^+$ (Figure 1 ▽) is observed. Also, a fragment signal corresponding to the stoichiometry $Au(C_2H_4)(CH_4)^+$ (Figure 1 *, mass signal not shown in Figure 1b) appears at 250 K.

A further increase of the ion-trap temperature to 270 K leads to the product ion mass distribution displayed in Figure 1c. Most importantly, the complex $Au_2(C_2H_4)^+$ (Figure 1 ◇) is detected but the product $Au_2(CH_4)_2^+$ (Figure 1 ○) almost completely disappeared. Finally, at room temperature (Figure 1d), only the product ions $Au_2(CH_4)^+$, $Au_2(C_2H_4)^+$, and the fragment $Au(C_2H_4)(CH_4)^+$ (not shown) remain.

To deduce a reaction mechanism from the measurements, we also considered the temperature-dependent kinetic data shown in Figure 1e–g. A reaction mechanism that best fits these kinetics and which has been formulated in conjunction with our first-principles theoretical modeling (see below), is shown in Scheme 1. The fit of the integrated rate equations of this mechanism to the experimental data is represented by the solid lines in Figure 1e–g.[14] The first step of this reaction mechanism, the adsorption of one methane molecule to Au_2^+, is not part of the cycle, but $Au_2(CH_4)^+$ is re-formed through release of the C_2H_4 unit from $Au_2(C_2H_4)(CH_4)^+$. This reaction competes with the gold-dimer fragmentation reaction.[15] No equilibrium reactions are required for the individual steps of the cycle. In fact, any such change to the reaction mechanism shown in Scheme 1 leads to an inferior fit with the measured kinetic data.

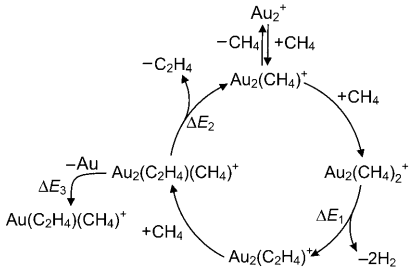

Scheme 1. Reaction mechanism that best fits the kinetic data.

The results of the fit that is obtained for the case where Au_2^+ is included in the reaction cycle are indicated by the dashed lines in Figure 1e for the product ions $Au_2(CH_4)^+$, $Au_2(C_2H_4)^+$, and $Au_2(C_2H_4)(CH_4)^+$. It is evident that with this assumption even a qualitative agreement cannot be achieved. In addition, if Au_2^+ was part of the reaction cycle, an offset in the Au_2^+ concentration would be expected for long reaction times, which is not observed.

From the temperature-dependent experiments we may assign energy barriers for processes included in the reaction mechanism. The first barrier ΔE_1 (see Scheme 1) is encountered in the dehydrogenation/H_2 elimination reaction step, and it is observed to be surpassed only at temperatures of 250 K and above. A second barrier (ΔE_2 in Scheme 1) must be involved in the release of C_2H_4 from $Au_2(C_2H_4)(CH_4)^+$ because this intermediate is observed at 250 and 270 K but not at 300 K, which implies that at this elevated temperature the barrier is easily surmounted and that the respective reaction step has become faster than the time scale of our experiment. Finally, a third barrier (ΔE_3 in Scheme 1) is connected to the fragmentation of the gold dimer.

The analysis of the kinetic data leading to the formulation of the reaction mechanism described above (Scheme 1) was guided by first-principles density-functional theoretical calculations (see Theoretical Method) which in addition provided deep insights into the nature of bonding of the reactant molecules and reaction intermediates to the gold cluster, and revealed the details (pathways and activation barriers) of the reaction mechanism.

The reaction profile (RP) leading to the catalytic production of ethylene, is shown in Figure 2, along with calculated atomic structures corresponding to reaction intermediates, transition states, and products.

A methane molecule adsorbs readily to Au_2^+ (adsorption energy $E_{ad} = 0.88$ eV), with the $C(sp^3)H_4$ orbitals overlapping with the d orbitals of the gold cluster; in the lowest energy configuration the methane molecule is bonded directly to one of the Au atoms, with two of the H atoms located closer to the gold atom (A in Figure 2). Adsorption of an additional CH_4 molecule leads to an additional gain of 0.57 eV (B in Figure 2 in which an H atom bridges each of the adsorbed molecules to the nearest Au atom).

The sequence of steps, starting with $Au_2(CH_4)_2^+$ (B in Figure 2) and leading to an ethylene molecule adsorbed on the gold cluster ($Au_2(C_2H_4)^+$, S in Figure 2, corresponding to the bottom of the reaction cycle in Scheme 1) are denoted as B to S in Figure 2, and they consist of local potential-energy minima connected by transition-state (TS) barriers, with atomic configurations corresponding to the minima and TS given, respectively, in the upper and lower rows in Figure 2. The TS encountered in the process of elimination of the first H_2 molecule is given by configuration I, and the subsequent local minimum corresponding to $Au_2(CH_3)_2^+$ is denoted by K. The second H_2 elimination TS barrier is denoted by R. The largest TS barriers in the RP leading to configuration S involve formation of "Au-insertion configurations" where an Au atom is inserted between a CH_3 group and an H atom (that

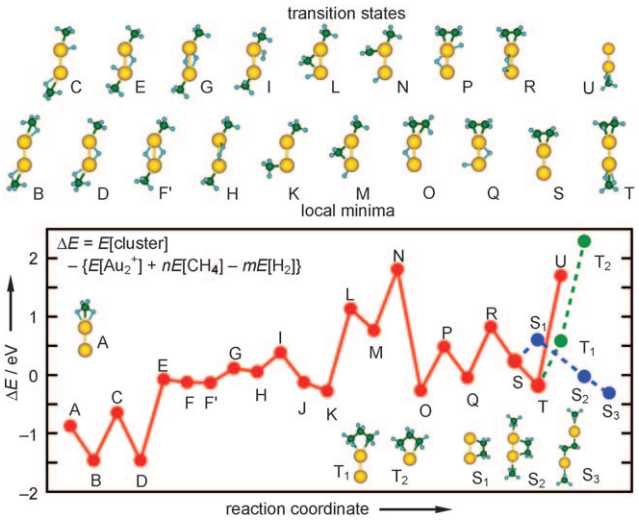

Figure 2. Calculated reaction pathways (see text for detail): Atomic configurations corresponding to transition state barriers and local potential energy minima are shown the top two rows (Au yellow, C green, H light blue). The pathway leading to formation and desorption of ethylene, ending with $Au_2(CH_4)^+$ (denoted as U) is connected by a solid line. Alternative pathways are denoted by dashed lines: T→T_2 (dashed green line) describes dissociation of the gold cluster; S→S_3 (dashed blue line), describes formation of $Au_2(C_4H_{12})^+$. All the species found in the mass spectra (Figure 1), and occurring in the reaction mechanism cycle (Scheme 1), are found on the calculated reaction path. For configuration U, the curly bracket should include {...−E[C_2H_4]}, and for T_2 it should include {...−E[Au]}.

is, the H atom is not bonded directly to the CH_3 group, see D, F′, and L), as well as "shuttle" (or "translocation") of a CH_2 group from one Au atom to another (see the transitions K→L→M→N). Interestingly, direct desorption of ethylene from the complex $Au_2(C_2H_4)^+$ is calculated to be unfeasible (requiring a very large activation energy). Instead, it proceeds via an intermediate in which a CH_4 molecule adsorbs first on the "unoccupied" Au atom ($Au_2(C_2H_4)(CH_4)^+$, configuration T) with subsequent desorption of C_2H_4, ending at the top of the cycle (configuration U, compare with Scheme 1). The exothermic nature of the hydrogen elimination (R→S) and methane addition (S→T) steps could trigger the cluster dissociation process (involving migration and rearrangement steps as depicted by T→T_1→T_2 in Figure 2, see left branch in Scheme 1. The calculated cluster dissociation energy, T_1→T_2, is 1.71 eV, compared with 2.46 eV for bare Au_2^+). We also include in Figure 2, an alternative low-barrier reaction path (S→S_1→S_2→S_3) that leads to formation of an adsorbed higher hydrocarbon with a stoichiometry of $Au_2(C_4H_{12})^+$ (which, as mentioned above has been observed as a low-intensity product). However this reaction path will terminate the catalytic cycle because the gold–gold bond is broken.

In conclusion, we report joint theoretical simulations and gas-phase ion-trap reaction kinetics measurements that reveal new catalytic methane activation and C–C bond formation mechanisms with an isolated gold dimer ion as a catalyst. It is noteworthy that for both the C–H bond activation and subsequent ethylene release processes the cooperative action of multiple molecules adsorbed on the cluster was found to be most effective. Methodologically, this research effort demonstrates the ability to gain deep insights about complex cooperative chemical reaction processes through a coordinated application of state-of-the-art experimental and first-principles theoretical techniques to judiciously chosen model catalytic systems, resulting in the elucidation of detailed reaction mechanisms (Figure 2) and formulation of a catalytic cycle (see Scheme 1) which are of fundamental, as well as of potential practical, interest.

Experimental Section

Experimental Method: The experiments were carried out using a variable temperature RF octopole ion trap inserted into a tandem quadrupole mass spectrometer as described elsewhere.[16] Briefly, the gold clusters are generated in a sputtering ion source.[17] The clusters are mass selected in a first quadrupole and then guided into the octopole ion trap. The ion trap is attached to a helium cryostat that allows for temperature adjustment in the range between 20 K and 300 K. The trap is prefilled with about 1 Pa partial pressure of helium buffer gas and a small, well-defined fraction of CH_4. Thermal equilibration of the clusters is achieved within a few milliseconds (about 10^3 collisions) under our experimental conditions, while the clusters are stored for a considerably longer time, typically between 0.1 s and several seconds.[16] After a chosen reaction time, all ionic reactants, intermediates, and products are extracted from the ion trap, and the ion distribution is mass analyzed by a second quadrupole mass filter. By recording all the ion intensities as a function of reaction time, that is, the storage time, the kinetics at a well defined reaction temperature can be obtained.

Theoretical Method: The theoretical explorations of the atomic arrangements and electronic structures of Au_2^+ and its complexes with the methane molecules along the reaction paths have been performed with first-principles density functional theory (DFT) calculations. In particular, we employed the Born–Oppenheimer (BO)—spin density functional (SDF)—molecular dynamics (MD) method, BO-SDF-MD[18] with norm-conserving soft pseudopotentials (including a scalar relativistic pseudopotential for Au)[19] and the generalized gradient approximation (GGA)[20] for electronic exchange and correlations. In these calculations we have used a plane-wave basis with a kinetic-energy cutoff of 62 Ry. The BO-SDF-MD method is particularly suitable for investigations of charged systems since it does not employ a supercell (i.e., no periodic replication of the ionic system is used). Structural optimizations were performed using a conjugate-gradient-like method.

In the first-principles calculations of the reaction profiles (pathways) a reaction coordinate was judiciously chosen; the reaction coordinate may consist of several geometrical parameters pertinent for the studied mechanism—for example, a reaction coordinate may entail, at a certain stage, the distance between two reacting atoms, such as, the distance between an H atom of an adsorbed methane molecule and the nearest Au atom, while at a subsequent stage of the reaction the pertinent reaction coordinate may correspond to the rotation angle of a chosen molecular group. For each value of the reaction coordinate, the total energy of the system was optimized through unconstrained relaxation of all of the other degrees of freedom of the system (reactant molecules and gold cluster atoms). The reaction profiles were obtained by repeating such calculations for various values of the chosen reaction coordinate.

Received: October 8, 2009
Revised: November 2, 2009
Published online: January 5, 2010

Keywords: ab initio calculations · catalysis · cluster compounds · gas-phase reactions · gold

[1] G. A. Olah, A. Goepper, G. K. S. Prakash, *Beyond Oil and Gas: The Methanol Economy*, Wiley-VCH, Weinheim, **2006**.
[2] S. J. Blanksby, G. B. Ellison, *Acc. Chem. Res.* **2003**, *36*, 255.
[3] R. H. Crabtree, *J. Organomet. Chem.* **2004**, *689*, 4083.
[4] D. K. Böhme, H. Schwarz, *Angew. Chem.* **2005**, *117*, 2388; *Angew. Chem. Int. Ed.* **2005**, *44*, 2336.
[5] *Nanocatalysis* (Eds.: U. Heiz, U. Landman), Springer, Berlin, **2007**.
[6] G. C. Bond, C. Louis, D. T. Thomson, *Catalysis by Gold*, Imperial College Press, London, **2006**; U. Landman, B. Yoon, C. Zhang, U. Heiz, M. Arenz, *Top. Catal.* **2007**, *44*, 145.
[7] A. Sanchez, S. Abbet, U. Heiz, W.-D. Schneider, H. Häkkinen, R. N. Barnett, U. Landman, *J. Phys. Chem. A* **1999**, *103*, 9573.
[8] H. Häkkinen, U. Landman, *J. Am. Chem. Soc.* **2001**, *123*, 9704; T. M. Bernhardt, U. Heiz, U. Landman in *Nanocatalysis* (Eds.: U. Heiz, U. Landman), Springer, Berlin, **2007**, and references therein.
[9] D. Schröder, H. Schwarz, *Proc. Natl. Acad. Sci. USA* **2008**, *105*, 18114; D. Schröder, J. Hrušák, R. H. Hertwig, W. Koch, P. Schwerdtfeger, H. Schwarz, *Organometallics* **1995**, *14*, 312.
[10] K. K. Irikura, J. L. Beauchamp, *J. Phys. Chem.* **1991**, *95*, 8344; F.-X. Li, P. B. Armentrout, *J. Chem. Phys.* **2006**, *125*, 133114.
[11] K. Koszinowski, D. Schröder, H. Schwarz, *J. Chem. Phys. A* **2003**, *107*, 4999.
[12] K. Koszinowski, D. Schröder, H. Schwarz, *ChemPhysChem* **2003**, *4*, 1233.
[13] D. M. Cox, R. Brickman, K. Creegan, A. Kaldor, *Z. Phys. D* **1991**, *19*, 353; D. M. Cox, R. Brickman, K. Creegan, A. Kaldor, *Mater. Res. Soc. Symp. Proc.* **1991**, *206*, 43.
[14] For the evaluation of the integrated rate equations of a proposed mechanism a least-squares fitting procedure was employed implemented in the chemical kinetics evaluation software DETMECH; E. Schumacher, University of Bern, Chemistry Department, **2003**.
[15] It has to be noted that the gold-dimer fragmentation might also proceed from $Au_2(C_2H_4)^+$ to yield $Au(C_2H_4)^+$ which might further react with a methane molecule faster than the time scale of our experiment to produce the observed fragment $Au(C_2H_4)(CH_4)^+$. This alternative would not be distinguishable in the reaction kinetics.
[16] T. M. Bernhardt, *Int. J. Mass Spectrom.* **2005**, *243*, 1.
[17] R. Keller, F. Nöhmeier, P. Spädtke, M. H. Schönenberg, *Vacuum* **1984**, *34*, 31.
[18] R. N. Barnett, U. Landman, *Phys. Rev. B* **1993**, *48*, 2081.
[19] N. Troullier, J. L. Martins, *Phys. Rev. B* **1991**, *43*, 1993.
[20] J. P. Perdew, K. Burke, M. Ernzerhof, *Phys. Rev. Lett.* **1996**, *77*, 3865.

